

# We are IntechOpen, the world's leading publisher of Open Access books Built by scientists, for scientists

6,900

Open access books available

186,000

International authors and editors

200M

Downloads

Our authors are among the

154

Countries delivered to

TOP 1%

most cited scientists

12.2%

Contributors from top 500 universities



WEB OF SCIENCE™

Selection of our books indexed in the Book Citation Index  
in Web of Science™ Core Collection (BKCI)

Interested in publishing with us?  
Contact [book.department@intechopen.com](mailto:book.department@intechopen.com)

Numbers displayed above are based on latest data collected.  
For more information visit [www.intechopen.com](http://www.intechopen.com)



# Development of Functionally Gradient Cu-Sn-Ni Alloy Using GTA Heat Source

*Cherian Paul and Ramasamy Sellamuthu*

## Abstract

The impact of nickel content on surface hardness, microstructure and wear properties of surface alloyed Cu-10Sn bronze composite was examined in this chapter. Gas Tungsten Arc (GTA) was utilized as the heat source for the surface alloying/modification process. The surface modification process was carried out on bronze samples coated with various Nickel coating thicknesses. Vickers hardness tester was used to measure the surface hardness as well as the hardness along the depth of the modified layer and wear rate was measured using a pin-on-disc tribometer. The Ni concentration profiling was carried out using EDAX. Surface modification process resulted in the formation of a layered functionally graded bronze alloy. The average grain size was found to reduce upon surface modification process. Ni addition was observed to increase the hardness and reduce wear rate for the modified samples.

**Keywords:** nickel profile, heat source, functionally graded material, FGM, hardness, wear behavior, surface modification

## 1. Introduction

Bronze, owing to its superior wear resistance is generally treated as one of the most commonly used engineering materials mainly as a bearing material in aerospace, automotive as well as industrial applications. Researches are being conducted on application of traditional coating methods like PVD, CVD, sputter deposition, electroplating, etc., for improving the surface properties of bronze. Surface modification process (SMP) has become an emerging technique to replace the traditional coating processes to improve the tribological properties of ferrous as well as non-ferrous alloys. In SMP, a heat source is used to melt the substrate surface and thereby a molten pool is formed. Then, the heat source is progressively moved along the length of the substrate so that, upon solidification a modified layer will be formed. In the case of fixed heat source, substrate will be moved. The major advantage of using SMP is that, the modified layer formed after solidification is integral to the substrate Benkisser et al. [1]. The applications of the alloys can be extended to ship propellers, sub-sea weapon ejection system, pumps, bearings and bushes as well. The drawback of traditional coatings getting delaminated on repeated cycles of operation can be omitted by using SMP. The formation of a functionally graded material (FGM) can be expected as a result of SMP. Since FGM is characterized by the gradual variation in composition and structure over volume, SMP with alloying elements results in the formation of an FGM. Wear

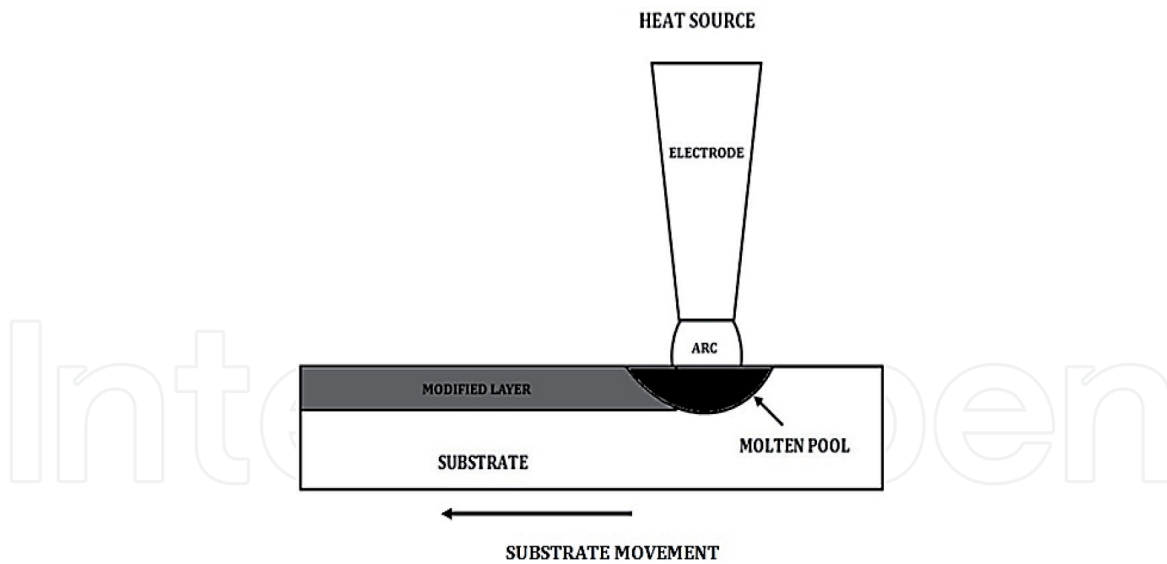


**Figure 1.**  
Surface modification process.

Process variable	Value	Unit
Current	200	A
Electrode diameter	2.4	mm
Arc length	1.5	mm
Electrode angle	180	°
Traverse speed	1	mm/s
Argon flow rate	12	l/min

**Table 1.**  
GTA process variables.



**Figure 2.**  
Experimental setup.

resistance, hardness, corrosion resistance, thermal conductivity, etc., of various alloys can be improved by the application of SMP. C Paul [2]. A schematic of SMP is shown in **Figure 1**.

This chapter discusses an investigation on the effect of Ni content on the hardness, the wear rate and the coefficient of friction of the surface alloyed Cu-Sn bronze alloy. As no previous works have been reported in the literature on the effect of Ni content on the hardness and the wear behavior of the surface alloyed bronze alloy, the present research work is undertaken. In the present study, the Sn content of the alloy was kept constant at 10 wt % and the Ni content was varied. The bronze substrates are coated with Ni of varying coating thickness (80, 120, 160 and 200  $\mu\text{m}$ ) using electroplating technique. The surface alloying process was carried out on the Cu-Sn bronze alloy coated with Ni. The GTA was used as the heat source. The GTA process variables, current (I), electrode diameter ( $e\Phi$ ), arc length (l), electrode angle ( $e\theta$ ), traverse speed (u) and argon flow rate are kept constant during the surface alloying process. The GTA process variables used in this study are reported in **Table 1**. The Ni concentration profiling was carried out for the surface alloyed samples. The Ni concentration was measured on the surface as well as along the depth of the modified layer formed in the surface alloying process using EDAX

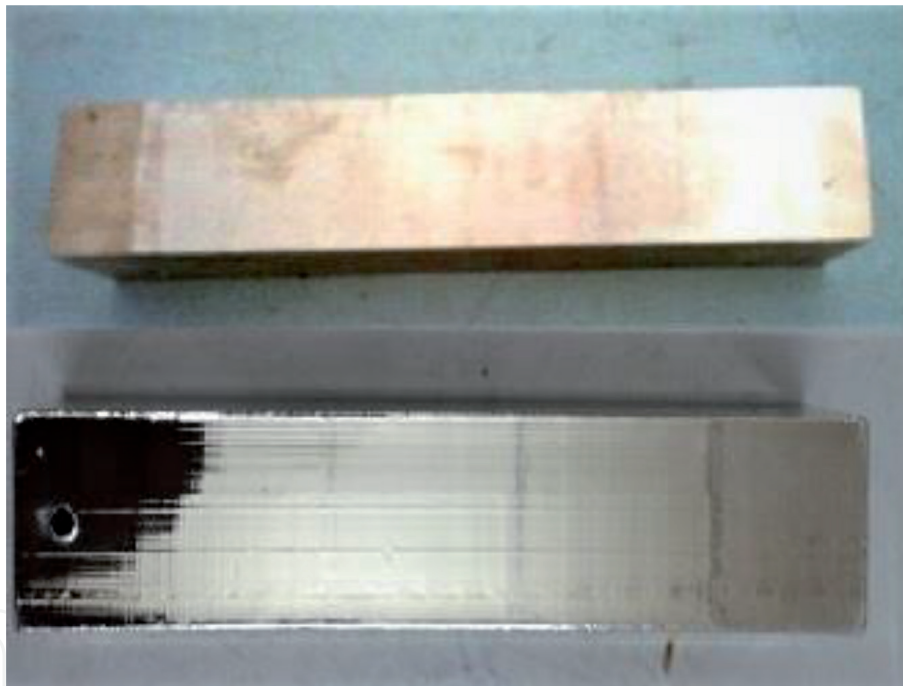


**Figure 3.**  
*Cu-Sn alloy with and without Ni coating.*



**Figure 4.**  
*Cu-Sn alloy surface modified with Ni.*

analysis. Microstructural examination, hardness measurement and wear measurements were carried out for the substrate and for the specimen surface alloyed with Ni. **Figure 2** shows the experimental setup.

**Figure 3** shows the Cu-Sn alloy substrate with and without Ni coating and **Figure 4** shows the surface modified Cu-Sn-Ni alloy.

## 2. Microstructural examination

A typical dendritic structure was observed in the as-cast substrate of Cu-10Sn bronze alloy as shown in **Figure 5** and the microstructure of the Ni surface alloyed Cu-10Sn alloy is shown in **Figure 6**.

It can be observed from **Figure 6** that the structure is very fine as opposed to a coarse structure observed in **Figure 5** and therefore it can be concluded that the grain refinement occurs as a result of the surface alloying process [3]. This refinement is due to the fast cooling experienced during solidification in the surface alloying process. A similar fine grained microstructure was observed for all the other Ni alloyed specimens also. Yilbas et al. [4, 5] studied the effect of laser surface modification treatment of aluminum bronze (Cu-9%Al-3%Fe) with

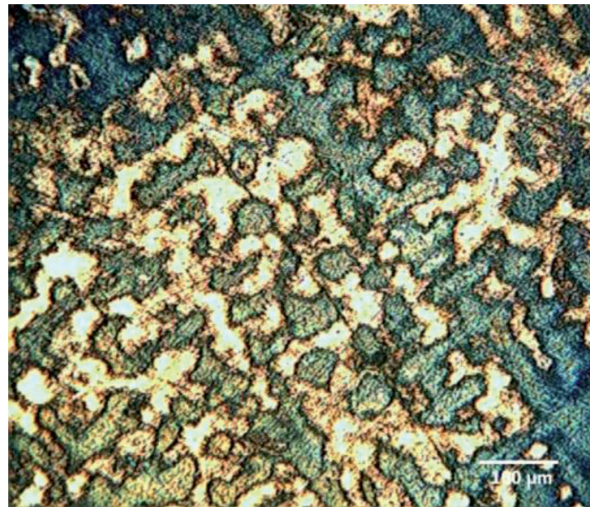


**Figure 5.**  
*As-cast Cu-Sn.*

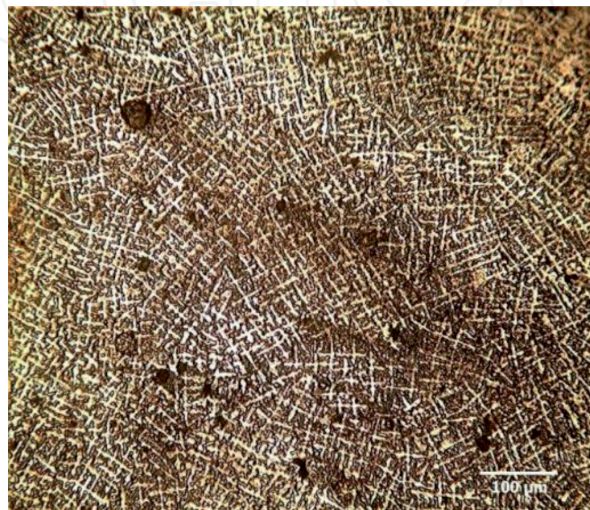


**Figure 6.**  
*Ni surface alloyed Cu-Sn.*

B4C and reported that fine grains are formed at the laser treated surface in the surface modification process because of high cooling rate. Kac et al. [6] studied the structure and properties of surface alloyed aluminum bronze (Cu-10%Al-4%Fe-2%Mn) with Ti as the alloying element using laser heat source. They reported that a very fine microstructure was formed in the rapid solidification experienced in the laser process. Viswanadham et al. [7] studied the injection of TiC particles into aluminum bronze (Cu-7%Al-3%Fe-1.5%Mn) using the laser as the heat source. They have reported that the modified layer in the laser treated specimen was found to be dense and highly uniform when compared to the untreated specimen. Majumdar and Manna [8] carried out the surface alloying of pure Cu with Cr using the laser as the heat source and they have evaluated the microstructure resulting from the surface alloying process. They reported that the microstructure of the alloyed zone changed from coarse dendritic for the substrate to a fine dendritic structure in the surface alloying process. It can be concluded that the result obtained in the present study is consistent with that of the previous studies.

### 3. Ni concentration profile

The Ni concentration on the surface of the modified layer formed in the surface alloying process was measured using the EDAX analysis. The concentration along the depth of the modified layer was also measured. **Figure 7** shows the points where the Ni concentration was measured. The Ni peaks can be observed in the EDS spectrum for all the surface alloyed specimen and the spectrum for 200  $\mu\text{m}$  Ni is shown in **Figure 8**.

Further, the results obtained by the EDAX analysis are reported in **Table 2**.

The Ni concentration values (wt %) reported in **Table 2** are plotted against the distance along the depth of the modified layer. **Figure 9** shows the Ni profiles for various coating thickness.

It can be observed from **Figure 9** that the Ni concentration is found to be the maximum on the surface of the modified layer for all the coating thickness. The Ni concentration decreases along the depth of the modified layer for all the coating thickness. It can be clearly observed that a gradient exists in the Ni concentration profile.

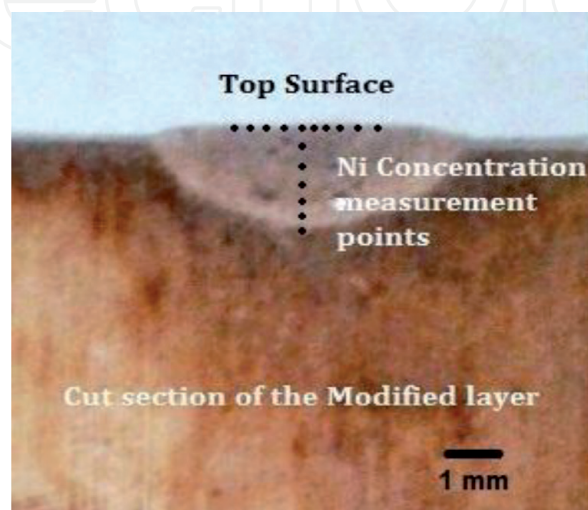


**Figure 7.**  
*Ni concentration measurement points.*

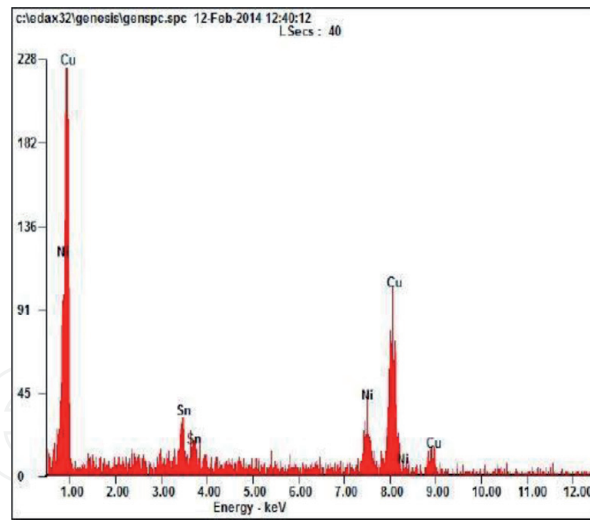


**Figure 8.**  
EDS spectrum for 200  $\mu\text{m}$  Ni coated samples.

Depth from the top surface (mm)	Ni concentration for various coating thicknesses (wt %)			
	80 $\mu\text{m}$	120 $\mu\text{m}$	160 $\mu\text{m}$	200 $\mu\text{m}$
0	5.03	8.53	13.61	17.81
0.3	4.9	8.39	12.92	14.88
0.6	4.48	7.15	10.18	13.65
0.9	3.26	6.46	7.86	10.41
1.2	2.95	5.83	6.85	7.35
1.5	2.15	4.36	5.02	5.89
1.8	0.87	2.48	3.15	4.26

**Table 2.**  
Ni concentration along the depth of the modified layer for four coating thickness.

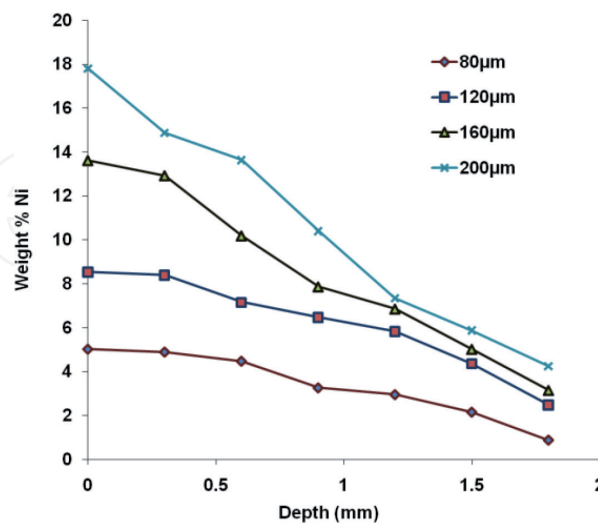


**Figure 9.**  
Ni concentration profile.

#### 4. Micro-hardness

The surface hardness values of the substrate and the surface alloyed specimens with varying Ni concentration were measured. Several readings were taken at

different locations and an average value was calculated. The surface hardness increased from 120 HV for the substrate to 485 HV for the specimen surface alloyed with a Ni coating thickness of 200  $\mu\text{m}$ . The average surface hardness values of the substrate and the Ni surface alloyed specimens are reported in **Table 3**.

The variation in the surface hardness with the Ni concentration is shown in **Figure 10**. It can be observed that the hardness increases with an increase in the Ni concentration. Ni contributes significantly to the hardness of the Cu-10Sn bronze alloy. The increase in the hardness is attributed to the presence of Ni in the solid solution. Hence, the hardening mechanism is solid solution strengthening.

Hardness values are measured at different points along the depth of the modified layer and are reported in **Table 4** and are represented graphically in **Figure 11**.

The hardness is found to decrease along the depth direction for all the surface alloyed specimen as shown in **Figure 11**. It can be concluded that a gradient exists in the hardness profile along the depth direction. The gradient so observed is attributed to the variation in the Ni concentration along the depth of the modified layer (refer to **Table 2**). The hardness is found to be the maximum for a concentration of 17.8 wt % Ni. It can be inferred that the hardness on the surface of the modified layer formed in the surface alloying process can be controlled by controlling the Ni concentration. Kac et al. [6] studied the structure and properties of Cu-10%Al-4%Fe-2%Mn bronze with an addition of Ti on the surface using laser as the heat source. They reported that a gradient exists in hardness along the depth direction of the modified layer. The observation obtained is consistent with that of Kac et al. [6].

**Figure 12** is a bar chart showing the hardness values obtained for the substrate, surface refined and the Ni surface alloyed specimens. It can be observed that the

Alloy	Ni coating thickness ( $\mu\text{m}$ )	wt % Ni	Hardness (HV0.1)	
			Substrate	Surface alloyed with Ni
Cu-10Sn	80	5.03	120	326
Cu-10Sn	120	8.53	120	379
Cu-10Sn	160	13.61	120	418
Cu-10Sn	200	17.81	120	485

**Table 3.**  
 Hardness values.

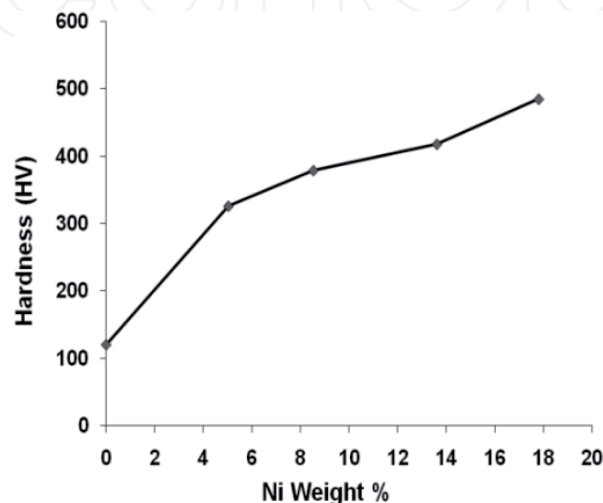


**Figure 10.**  
 Hardness variation with Ni concentration.

Depth (mm)	Hardness for various Ni coating thickness (HV0.1)			
	80 $\mu\text{m}$	120 $\mu\text{m}$	160 $\mu\text{m}$	200 $\mu\text{m}$
0	326	379	418	485
0.25	289	361	410	478
0.5	268	347	389	431
0.75	248	311	365	399
1	201	289	321	347
1.25	189	240	266	314
1.5	166	201	227	269
1.6	154	182	213	244
1.8	140	162	197	223
1.85	120	147	184	120
1.9	120	120	120	120

**Table 4.**  
Hardness along the depth of the modified layer for various Ni coating thickness.

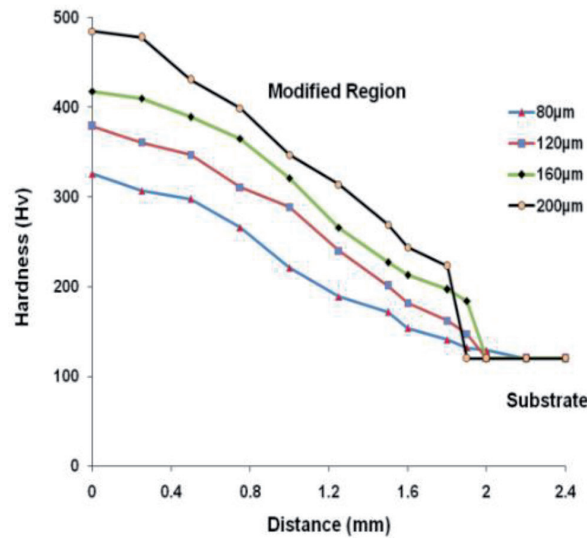


**Figure 11.**  
Hardness profile.

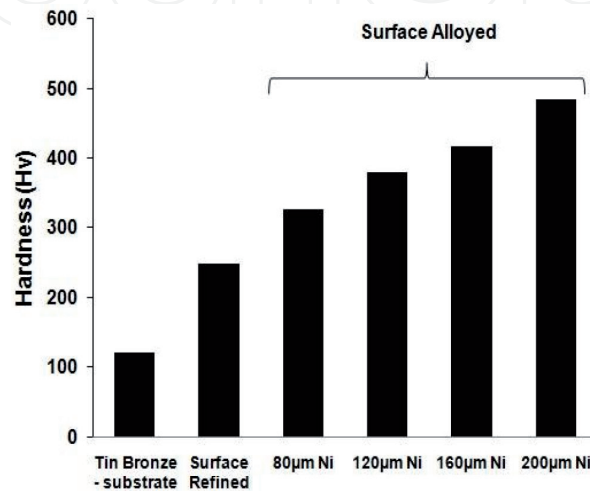


**Figure 12.**  
Hardness values—substrate, surface refined and Ni surface alloyed specimen.

surface refining process and the surface alloying process significantly increases the hardness of the alloy. Increase in hardness observed in the surface refining process is attributed to the formation of fine grained microstructure due to rapid solidification in the surface refining process. However, the grain refinement occurs in the surface alloying process as shown in **Figure 6**. The addition of Ni in the surface alloying process also contributes to the improvement in the hardness of the alloyed specimen as shown in **Figure 11**. Hence, the increase in hardness is attributed to the grain refinement occurring in the surface alloying process and also to the Ni addition.

## 5. Wear behavior

A typical height loss vs. time plot for the Cu-10Sn modified alloy is shown in **Figure 13**. It can be observed that the height loss increases linearly with the sliding time. This behavior is in agreement with the results reported by Singh et al. [9] in the bulk alloys.

The wear results obtained for the substrate and the Ni surface alloyed samples are reported in **Table 5**.

It can be observed that the wear rate reduced significantly after surface alloying with Ni. The reduction in the wear rate is attributed to the increase in the hardness after Ni addition.

**Figure 14** is a bar chart showing the variation in the wear rate with the Ni concentration. It can be observed that the wear rate decreases with an increase in the Ni concentration. The minimum wear rate was obtained for the 17.8 wt % Ni. It can be concluded that the wear rate of the Cu-Sn bronze alloy can be reduced by surface alloying with Ni. The increased hardness due to the Ni addition is the reason behind the reduction in the wear rate.

**Figure 15** is a bar chart showing the wear rate obtained for the substrate, surface refined and the Ni surface alloyed specimens.

It can be observed from **Figure 15** that the surface refining process decreases the wear rate marginally and the surface alloying process remarkably decreases the wear rate of the Cu-10Sn bronze alloy. The reduction in the wear rate observed in the surface refining process is due to the increase in the hardness as a result of the grain refinement due to the faster cooling rate experienced. Further, it is to be noted that the refinement in the grain structure also occurs in the surface alloying process

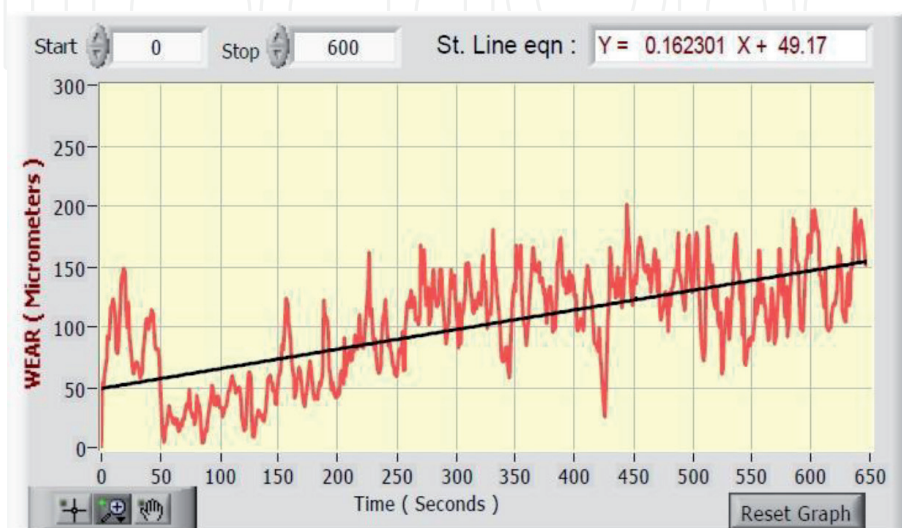


**Figure 13.**  
*A typical wear plot.*

as discussed earlier. However, the Ni addition significantly contributes to the increase in the hardness that reduces the wear rate of the surface alloyed specimen. Hence, the reduction in the wear rate is attributed to both the grain refinement occurring in the surface alloying process and the Ni addition.

A typical image showing the wear tracks after the dry sliding test on pin-on-disc wear tester for the Ni surface alloyed specimen is shown in **Figure 16**.

It can be observed from **Figure 16** that the wear mechanism is of adhesive type. Zhang et al. [10] studied the dry sliding wear behavior in the bulk Cu-15Ni-8Sn alloy. They reported that the adhesive wear took place under the dry sliding test

Substrate alloy	Ni coating thickness ( $\mu\text{m}$ )	Wear rate ( $\times 10^{-4} \text{ mm}^3/\text{m}$ )	
		Substrate	Surface alloyed
Cu-10Sn	80	18.40	13.70
Cu-10Sn	120	18.40	8.40
Cu-10Sn	160	18.40	4.5
Cu-10Sn	200	18.40	2.2

**Table 5.**  
Wear rate results.

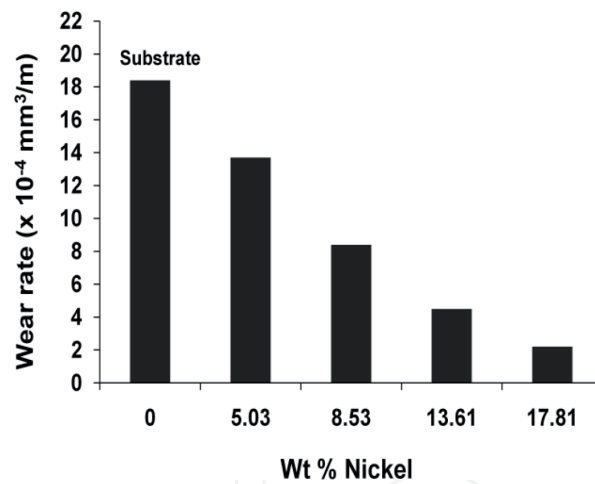


**Figure 14.**  
Variation in wear rate with Ni concentration.

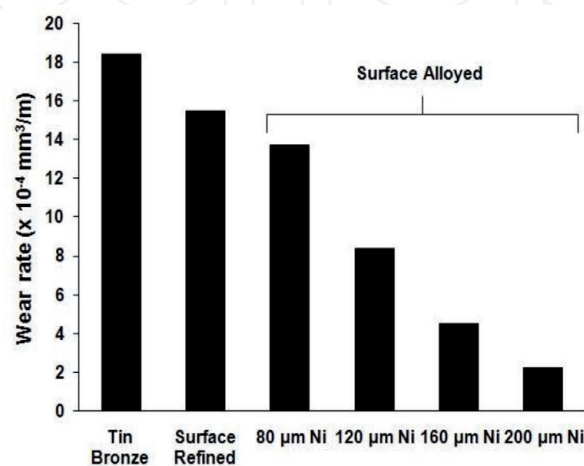


**Figure 15.**  
Wear rate—substrate, surface refined and surface alloyed specimens.

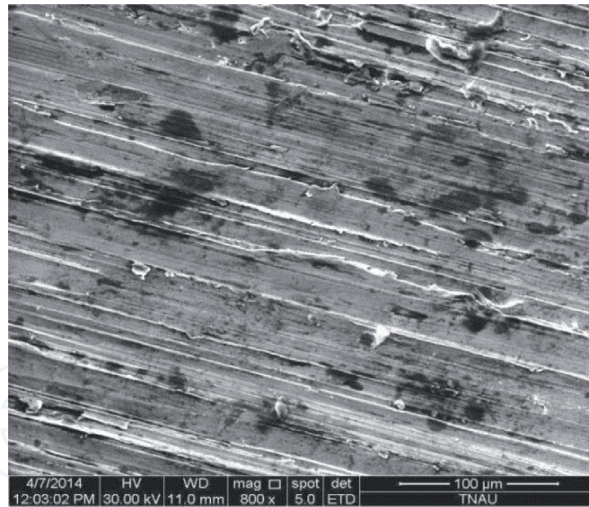


**Figure 16.**  
*Wear tracks.*

conditions. It is to be noted that the compositions of the modified layer in this study are similar to the Cu-15Ni-8Sn alloy that was used in the study of Zhang et al. Therefore, the observation in the present study is consistent with that of Zhang et al. [11].

## 6. Coefficient of friction

Frictional force vs. time plot of Ni Surface Alloyed Cu-10Sn alloy is shown in **Figure 17**. The same trend was found for all the other Ni Surface alloyed specimens.

It can be noticed that the frictional force becomes constant after a short period of time and remains as such. The rapid increase in frictional force found initially is due to the uneven contact between the modified specimen and counter face material. The frictional force remains constant once perfect contact is achieved. A typical plot of coefficient of friction vs. time for the surface alloyed Cu-10Sn alloy is shown in **Figure 18**. The plot shows both transient period and single steady-state regime. The reasons for the transient behavior may be the effect of work-hardening and/or accumulation of debris as reported by Singh et al. [9].

The coefficient of friction obtained in this study for the substrate and the surface alloyed Cu-10Sn alloys are reported in **Table 6**. An average value of 0.23 was obtained as frictional coefficient after surface alloying process.

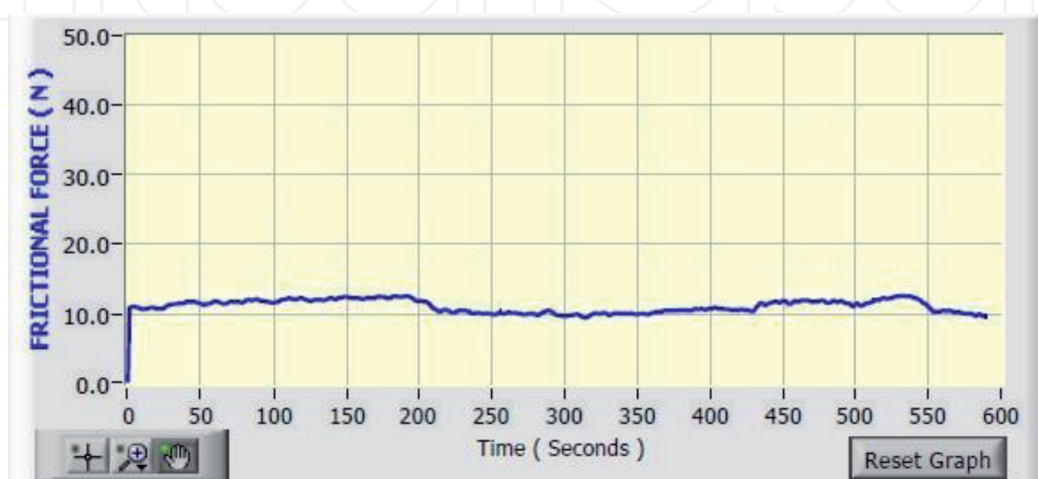


**Figure 17.**  
*Frictional force vs. time plot.*



**Figure 18.**  
COF vs. time plot.

Substrate alloy	Ni coating thickness ( $\mu\text{m}$ )	Coefficient of friction	
		Substrate	Surface alloyed
Cu-10Sn	80	0.27	0.24
Cu-10Sn	120	0.27	0.22
Cu-10Sn	160	0.27	0.23
Cu-10Sn	200	0.27	0.22

**Table 6.**  
Frictional coefficients for substrate and surface alloyed specimens.

Substrate alloy	Ni coating thickness ( $\mu\text{m}$ )	Hardness (HV0.1)	Coefficient of friction
Cu-10Sn	80	326	0.24
Cu-10Sn	120	379	0.22
Cu-10Sn	160	418	0.23
Cu-10Sn	200	485	0.22

**Table 7.**  
Coefficient of friction with hardness of the alloys.

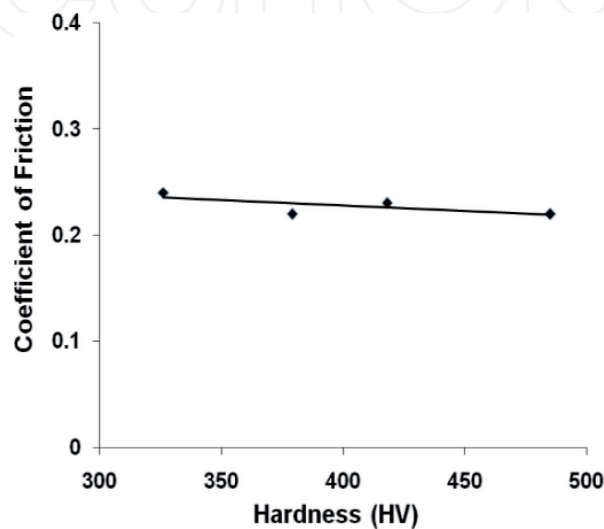


**Figure 19.**  
COF variation with hardness.

The hardness values and the coefficient of friction of surface alloyed Cu-10Sn bronze alloys are reported in **Table 7**.

**Figure 19** shows the variation in coefficient of friction with hardness for the Cu-10Sn bronze alloys surface alloyed with Ni. It can be inferred that the COF remains almost a constant value irrespective of the hardness.

## 7. Conclusions

Cu-10Sn Bronze alloy was Surface Alloyed with Ni and a functionally graded Cu-Sn-Ni alloy with superior surface hardness and wear resistance was developed. Based on the results of this investigation, the following conclusions are drawn:

- Refinement in grain structure occurs in the surface alloying process.
- A gradient exists in the Ni concentration profile along the depth direction of the modified layer formed in the surface alloying process.
- Hardness can be significantly improved by surface alloying with Ni.
- A gradient exists in the hardness profile along the depth direction of the modified layer formed in the surface alloying process.
- Hardness on the surface can be easily controlled by controlling the Ni concentration on the surface of the modified layer.
- The wear rate was found to decrease with increase in hardness, a finding consistent with Archard's theory and that of the previous studies.
- Addition of Ni is found to be highly effective in increasing the hardness of the parent substrate and reducing the wear rate when compared to the addition of other alloying elements like Ti, TiC and Cr.
- The wear behavior is found to be adhesive in nature.
- The Coefficient of Friction of the Surface Alloyed specimen is found to remain constant irrespective of the hardness.

## Acknowledgements

The author is deeply indebted to Defence Research Development Organization, New Delhi (DRDO) for the financial support provided for conducting this project (Project No: ERIP/ER/1003934/M/01/1345 dated 26 July 2011).

IntechOpen

## **Author details**

Cherian Paul<sup>1\*</sup> and Ramasamy Sellamuthu<sup>2</sup>

1 Department of Mechanical Engineering, SAINTGITS College of Engineering, Kottayam, Kerala, India

2 Department of Mechanical Engineering, Amrita School of Engineering, Amrita Vishwa Vidyapeetham, Coimbatore, Tamilnadu, India

\*Address all correspondence to: [cherian.paul@saintgits.org](mailto:cherian.paul@saintgits.org)

## **IntechOpen**

© 2019 The Author(s). Licensee IntechOpen. This chapter is distributed under the terms of the Creative Commons Attribution License (<http://creativecommons.org/licenses/by/3.0>), which permits unrestricted use, distribution, and reproduction in any medium, provided the original work is properly cited. 

## References

- [1] Benkisser G, Horn G, Semjonov S, Kaps R. Surface layer hardening of heterogeneous multialloy aluminium bronzes by laser beam melting. *Metall.* 1992;**46**(4):324-328
- [2] Paul C, Sellamuthu R. An investigation on the effect of process parameters on microstructure, hardness and wear properties of surface modified Cu-Sn bronze alloy. *Applied Mechanics and Materials.* 2014;**592-594**:58-62
- [3] Gadag SP, Galun R, Weisheit A, Mordike BL. Laser alloying of copper and its alloys. In: *Laser Processing: Surface Treatment and Film Deposition.* Vol. 307. 1996. pp. 359-377
- [4] Yilbas BS, Matthews A, Leyland A, Karatas A, Akhtar SS, Abdul Aleem BJ. Laser surface modification treatment of aluminium bronze with B<sub>4</sub>C. *Applied Surface Science.* 2012;**263**:804-809
- [5] Yilbas BS, Akhtar SS, Karatas C. Laser notriding of the surface of phosphor bronze. *International Journal of Advanced Manufacturing Technology.* 2013;**65**:1553-1565
- [6] Kac S, Kusinski J. Structure and properties of the bronze laser alloyed with titanium. *Applied Surface Science.* 2007;**253**:7895-7898
- [7] Viswanadham CS, Goswami GL, Galun R, Mordike BL. Laser melt injection of TiC particles into aluminium bronze. *Laser in engineering.* 2006;**16**:207-213
- [8] Majumdar JD, Manna I. Laser processing of materials. *Sadhana.* 2003;**28**(3&4):495-562
- [9] Singh JB, Cai W, Bellon P. Dry sliding of Cu-15 wt%Ni-8 wt%Sn bronze: Wear behaviour and microstructures. *Wear.* 2007;**263**:830-841
- [10] Zhang SZ, Jiang B, Ding WJ. Wear of Cu-15Ni-8Sn spinodal alloy. *Wear.* 2009;**264**(3-4):199-203
- [11] Zhang SZ, Jiang B, Ding WJ. Dry sliding wear of Cu-15Ni-8Sn alloy. *Tribology International.* 2010;**43**(1-2):64-68